The Ozonolysis of Ethylene: A Theoretical Study of the Gas-Phase Reaction Mechanism

Josep M. Anglada,*[a] Ramon Crehuet,[a] and Josep Maria Bofill[b]

Abstract: The gas-phase reaction mechanism of ethylene ozonolysis has been investigated from a theoretical point of view. The formation of the ethylene primary ozonide (1,2,3-trioxolane, POZ) from the ozone–ethylene reaction is calculated to be exothermic by 49.2 kcal mol^{-1} with an activation energy of 5.0 kcal mol^{-1} at 0 K, in agreement with experimental estimates. We have found two different paths for the cleavage of POZ, namely a concerted and a stepwise mechanism. The concerted path leads to the formation of Criegee intermediates (carbonyl oxide–formaldehyde pairs), for which we have calculated an activation energy of 18.7 kcal mol^{-1} at 0 K. The non-concerted mechanism involves three different routes for the POZ decomposition, leading to the formation of Criegee intermediates with a computed activation energy of 21.6 kcal mol^{-1} at 0 K; to hydroperoxyacetaldehyde with a calculated activation energy of 22.8 kcal mol^{-1} at 0 K; and to oxirane + excited molecular oxygen ($^1\Delta_g$) with a higher activation energy. Moreover, hydroperoxyacetaldehyde is formed with an excess of energy, so that it can decompose yielding OH radicals. The reaction of carbonyl oxide and formaldehyde produces the ethylene secondary ozonide (1,2,4-trioxolane, SOZ) and involves the formation of a van der Waals complex on the reaction coordinate, prior to the transition state. The process is calculated to be exothermic by 46.0 kcal mol^{-1} and the energy of the transition state is computed to be lower than that of the reactants: this process can therefore be considered barrierless. SOZ cleaves by a stepwise mechanism and we have found two different fates for its decomposition: dioxymethane + formaldehyde, and hydroxymethyl formate. The former is calculated to be endothermic by 33.3 kcal mol^{-1} with an energy barrier of 48.7 kcal mol^{-1}, whereas the tautomerization of SOZ leading to hydroxymethyl formate is highly exothermic (72.2 kcal mol^{-1}) and has an activation energy of 32.6 kcal mol^{-1} at 0 K. The unimolecular decomposition of dioxymethane, following three different paths, is also reported: dissociation into CO_2 + H_2, which is highly exothermic (111.6 kcal mol^{-1}) and has a low energy barrier (3.0 kcal mol^{-1}); isomerization to formic acid, also highly exothermic (101.9 kcal mol^{-1}) with a low activation energy (2.2 kcal mol^{-1} at 0 K); and radical fragmentation into H + HCOO, in a slightly endothermic process (4.9 kcal mol^{-1}) with an activation energy of 18.4 kcal mol^{-1} at 0 K. The dissociation of formic acid into H_2, CO_2, CO and H_2O and the decomposition of HCOO into H radicals + CO_2 are also discussed.

Keywords: ab initio calculations · ethylene · gas-phase chemistry · ozonolysis · reaction mechanisms

[a] Dr. J. M. Anglada, R. Crehuet
Institut d'Investigacions Químiques i Ambientals de Barcelona
Departament de Química Orgànica Biològica
CID – CSIC
C/Jordi Girona 18, E-08034 Barcelona (Spain)
Fax: (+34)93-2045904
E-mail: anglada@qteor.cid.csic.es
rcsqtc@cid.csic.es

[b] Dr. J. M. Bofill
Centre Especial de Recerca en Química Teòrica
Departament de Química Orgànica, Universitat de Barcelona
Martí i Franquès 1, E-08028-Barcelona (Spain)
E-mail: jmbofill@qo.ub.es

Introduction

The gas-phase reaction of ozone with olefins has received much attention in the last few years due to its importance in atmospheric chemistry, especially in air pollution processes in urban areas.[1–4] It is now generally accepted that the ozonolysis of olefins follows the mechanism proposed by Criegee,[5] which involves three main reactions; for ethylene these can be described as: a) formation of the ethylene primary ozonide (1,2,3-trioxolane, POZ) (1); b) decomposition of POZ into a carbonyl compound (formaldehyde) (2) and a carbonyl oxide (3) pair, commonly termed the Criegee intermediates; and c) cycloaddition of the carbonyl oxide to the carbonyl compound to yield the ethylene secondary ozonide (1,2,4-trioxolane, SOZ) (4).

Further experimental and theoretical investigations[6–14] indicate that the carbonyl oxide formed in the POZ cleavage can decompose unimolecularly following three alternative

pathways: i) the ester channel, which involves unimolecular isomerization to dioxirane, which subsequently decomposes into simpler species (H_2O + CO, H_2 + CO_2, 2 H + CO); ii) the hydrogen atom migration or hydroperoxide channel, for carbonyl oxides with α-hydrogen atoms, involving tautomerization to the corresponding hydroperoxide, which can decompose yielding OH radicals; iii) the oxygen-atom channel, involving the splitting off of $O(^3P)$ atoms after an intersystem crossing between the ground singlet state and the lowest triplet state of the carbonyl oxide.

Many investigations, both experimental and theoretical, of the ozonolysis of olefins have been undertaken.[4,15–39] The

Abstract in Catalan: *S'ha estudiat, des d'un punt de vista teòric, el mecanisme de la recció en fase gas de l'ozonòlisi de l'etilè. El càlcul de la formació de l'ozònid primari de l'etilè (1,2,3-trioxolà, POZ) inidica una exotermicitat de 49.2 kcal-mol^{-1} i una energia d'activació de 5.0 kcal mol^{-1} a 0 K, en acord amb estimacions experimentals. S'han trobat dos camins diferents per a la ruptura de l'ozònid primari: un de concertat i un de no-concertat. El concertat porta a la formació dels intermedis de Criegee (l'òxid de carbonil i el formaldehid), pel qual hem calculat una energia d'ativació de 18.7 kcal mol^{-1} a 0 K. El mecanisme no-concertat dóna lloc a tres possibles destins pel POZ: el primer, un camí que porta a la formació dels intermedis de Criegee amb una energia d'activació calculada de 21.6 kcal mol^{-1} a 0 K; el segon, que porta a l'hidroperoxiceltaldehid amb una energia d'activació calculada de 22.8 kcal mol^{-1} a 0 K; i el tercer, amb una energia d'activació més alta, que porta a oxirà més oxigen molecular en estat excitat ($^1\Delta_g$). A més a més, l'hidroperoxiacetaldehid es forma amb un excés d'energia, de manera que es pot descomposar produint radicals OH. La reacció de l'òxid de carbonil amb el formadehid dóna l'ozònid secundari de l'etilè (1,2,4-trioxolà, SOZ) i implica la formació d'un complex de van der Waals en la coordenada de reacció, previ a l'estat de transició. Segons els càlculs, aquest procés és exotèrmic en 46.0 kcal mol^{-1} i l'energia de l'estat de transició es troba per sota de la dels reactius. Per tant, aquest procés es pot considerar sense barrera. El SOZ es trenca en un mecanisme per etapes amb dos possibles camins que dónen dioximetà més formaldehid i formiat d'hidoximetil. La descomposició en dioximetà més formaldehid és endotèrmica en 33.3 kcal mol^{-1} amb una barrera energètica de 48.7 kcal mol^{-1}, mentre que la tautomerització de SOZ per donar formiat d'hidoximetil és altament exotèrmica (72.2 kcal mol^{-1}) i té una energia d'activació de 32.6 kcal mol^{-1} a 0 K. Finalment també es descriu la descomposició unimolecular del dioximetà. Aquesta espècie es descomposa per tres camins diferents: dissociació en CO_2 més H_2, que és altament exotèrmica (111.6 kcal mol^{-1}) i té una barrera energètica molt baixa (3.0 kcal mol^{-1}); isomerització a àcid fòrmic, també altament exotèrmica (101.9 kcal mol^{-1}) i amb una energia d'activació baixa (2.2 kcal mol^{-1} a 0 K); i fragmentació radicàlaia en H més HCOO, en un procés lleugerament endotèrmic (4.9 kcal mol^{-1}) i amb una energia d'activació de 18.4 kcal mol^{-1} a 0 K. També es descriu la dissociació de l'àcid fòrmic en H_2, CO_2, CO i H_2O i la descomposició de HCOO en el radical H més CO_2.*

1 (POZ)   2   3   4 (SOZ)
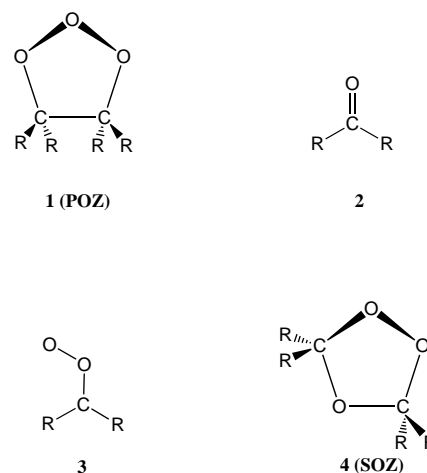
experimental investigations have shown that several products and intermediates of the ozonolysis of olefins are highly reactive. These can initiate secondary reactions, introducing uncertainties in the reaction mechanisms. Especially important is the hydroxyl radical (OH) that is produced in high yields in ozone – alkene reactions and reacts rapidly with alkenes and carbonyl compounds. Although several kinetic studies have provided rate constants of many reactions involved in the ozonolysis of olefins, other product studies suggest that the mechanism of these reactions is not fully understood.[31,34,35] Most of the theoretical work has been addressed to the study of carbonyl oxides and their unimolecular reactions.[11–14,40–44] Less attention has been paid to other reactions involved in the ozonolysis of olefins. In the early work of Wadt and Goddard[17] and Harding and Goddard[19] it was assumed that the decomposition of POZ is a stepwise process involving biradical intermediates, but the geometries of the postulated intermediates were not optimized and no transition structures were calculated. In contrast, other theoretical studies at both semi-empirical[29,37] and ab initio levels[18,23] suggest a concerted mechanism for the decomposition of POZ and SOZ. We believe that further theoretical study of the ozonolysis of olefins is necessary in order to elucidate the mechanism of the elementary reactions involved.

The aim of the present investigation was to perform a systematic theoretical study of the gas-phase mechanism of the reaction of ozone with ethylene by using high-level ab initio quantum chemical calculations. The study includes the formation of POZ from O_3 + C_2H_4, the subsequent decomposition of POZ and the formation and decomposition of SOZ. We have found that the cleavage of POZ yields the Criegee intermediates (carbonyl oxide and formaldehyde) [Eq. (1)], hydroperoxyacetaldehyde [Eq. (2)] and oxirane + O_2 in its $^1\Delta_g$ excited state [Eq. (3)]. Reaction (2) involves hydrogen atom 1,4-migration from carbon to oxygen. Since $CHOCH_2OOH$ is formed with an excess of energy, it can decompose into OH and $CHOCH_2O$ radicals.

The cleavage of SOZ takes place in a non-concerted mechanism that produces dioxymethane + formaldehyde [Eq. (4)], and hydroxymethyl formate [Eq. (5)].

$$(1)$$

$$(2)$$

$$(3)$$

$$(4)$$

$$(5)$$
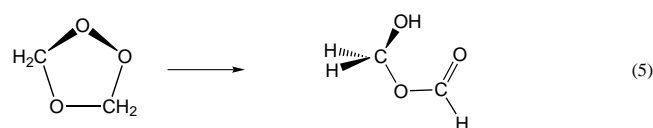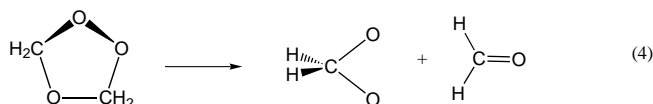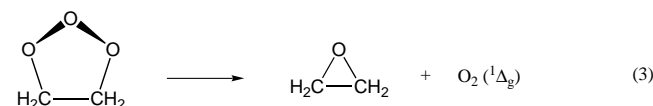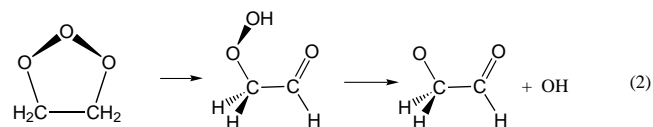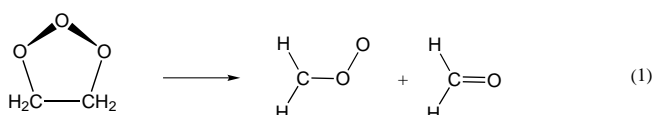
Dioxymethane is also an intermediate in the unimolecular decomposition of carbonyl oxide via dioxirane (in the so-called ester channel), and we have investigated its unimolecular decomposition into different products [Eq.(6)].

$$
\begin{cases}
H_2 + CO_2 \\
H_2O + CO \\
2H + CO_2
\end{cases}
\qquad (6)
$$
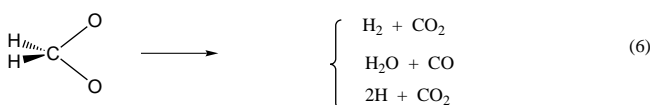
Computational Details

The molecular geometries of the stationary points located on the ground singlet state potential energy surfaces (PESs) were optimized by use of CASSCF wavefunctions[45] employing analytical gradient procedures.[46–48] The CASs were selected according to the fractional occupation of the natural orbitals (NOs)[49] generated from the first-order density matrix calculated from an MRD-CI[50–52] wavefunction, correlating all valence electrons. The active space composition changes according to the different reactions studied.[53] To compare the calculated geometries with other results from the literature, some stationary points involved in the formation and decomposition of POZ were also calculated using the DFT method[54–56] with Becke's three-parameter hybrid functional B3LYP.[57] Since many of these intermediates possess a strong biradical character, the B3LYP calculations were carried out with a UHF wavefunction of broken symmetry. Furthermore, the geometries of a few stationary points (formation of POZ and its concerted decomposition) were also calculated using the QCISD method.[58] The zero-point vibrational energies (ZPVEs) were determined from the CASSCF harmonic vibrational frequencies. The CASSCF ZPVEs were scaled by 0.8929.[59]

The split-valence-d-polarized 6-31G(d) basis set was used for the geometry optimizations,[60] except for the unimolecular decomposition of dioxymethane, for which the 6-31G(d,p) basis set[60] was employed.

The effect of the dynamic valence-electron correlation on the relative energy of the CASSCF-calculated stationary points was incorporated by performing single-point calculations by the QCISD(T) method.[58] In this case, the more flexible 6-311G(2d,2p) basis set[61] was used. In the decomposition of POZ, we found two particular cases where the quadratic configuration interaction calculations gave unreliable results. In these cases

we performed single-point calculations using the CCSD(T) method.[58,62,63] The 6-311G(2d,2p) basis set was also used in these calculations. For those structures showing a clear biradical character, the QCISD(T) and CCSD(T) calculations were based on a reference UHF wavefunction of broken symmetry. However, in some cases, the relative stability of the biradicals may have been underestimated because of spin contamination when a UHF reference function was used. Therefore some of the QCISD(T) and CCSD(T) single-point calculations were repeated over an RHF wavefunction (see the Supporting Information). The calculations were carried out using the GAMESS[64] and GAUSSIAN 94[65] program systems. Additionally, for the key structures with a clear biradical character in the POZ and SOZ decompositions, we performed further CASPT2[66] calculations, based on a common CASSCF(6,6) reference function, in order to compare the relative order of the energies of the different decomposition channels. The 6-311G(2d,2p) basis set was also used in these calculations, employing the Molcas version 2 package[67].

Throughout the text all geometric discussions refer to the CASSCF values and the relative energies considered are those obtained at CCSD(T) or QCISD(T) levels of theory. Because of the marked biradical character of several intermediates in the POZ and SOZ decompositions, a comparison of the energy barriers with those computed at the CASPT2 level of theory is also made for the key structures in the POZ and SOZ cleavage processes. Further comparisons with results obtained using other theoretical methods are included as Supporting Information. The Cartesian coordinates of the stationary points, the B3LYP, CASSCF, QCISD(T), CCSD(T) and CASPT2 absolute energies, and the dipole moments (calculated at the CASSCF level of theory) of all the structures reported in this paper are also available as Supporting Information.

Results and Discussion

The structures of the stationary points are designated by **M** for the minima and **TS** for the transition states, followed by a number (**1**, **2** and so on) indicating the order of introduction. The most relevant geometric parameters of the optimized structures for the stationary points are given in Figures 1, 3, 4 and 7. The computed relative energies and the ZPVEs are collected in Tables 1, 2 and 3 and schematic potential energy diagrams are presented in Figures 2, 5 and 6.

Formation of ethylene POZ **(1,2,3-trioxolane)**: The symmetry-allowed [4+2] cycloaddition of ozone to ethylene is the first step of the reaction. The process involves the formation of a van der Waals complex between O_3 and C_2H_4[68] along the reaction path prior to the transition state. Studies of this van der Waals complex, several conformations of POZ and the transition structure have been reported,[68–72] and we have focused our attention on the reactants, POZ (**M1**) and the transition structure (**TS1**) connecting the POZ with the van der Waals complex.

Our computed geometric parameters (Figure 1) are comparable with other results from the literature.[68,71–75] The most significant difference among the experimental values of **M1**[71] is in the C–O bond length, which is predicted to be 0.032 Å longer by our CASSCF calculations. Our calculations indicate that the formation of POZ (**M1**) is exothermic by 49.2 kcal mol^{-1} at 0 K (Table 1). This exothermicity is comparable with the experimental value of 45 ± 6 kcal mol^{-1} and other theoretical estimates (in the 43.7–57.3 kcal mol^{-1} range).[14,23,29,72] The activation energy relative to the reactants is computed to be 5.0 kcal mol^{-1} at 0 K. If we take into account the prediction from ab initio results in the literature that the
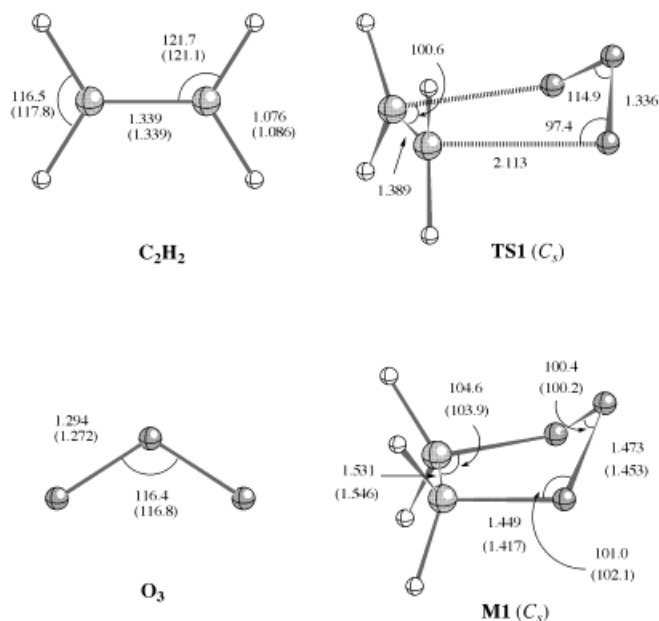
Figure 1. Selected geometric parameters of the CASSCF/6-31G(d)-optimized structures for the stationary points involved in the ethylene POZ formation. Distances are given in ångstroms and angles in degrees. Values in parentheses correspond to experimental data.

Table 1. Zero-point vibrational energies (ZVPE, [kcal mol^{-1}])[a] and relative energies (E [kcal mol^{-1}])[b,c] for the optimized structures involved in the formation and decomposition of Ethylene POZ.

Compound	ZPVE	E CCSD(T)/ 6–311G(2d,2p)
$O_3 + C_2H_4$	33.5	0.0 (0.0)
TS1	35.9	2.6 (5.0)
M1 (POZ)	39.5	− 55.2 (− 49.2)
TS2	38.8	− 34.9 (− 29.5)
M2	38.5	− 36.4 (− 31.4)
TS3	38.1	− 34.5 (− 29.8)
M3	38.3	− 37.3 (− 32.5)
TS4	36.5	− 33.5 (− 30.5)
TS5	36.4	− 30.5 (− 27.6)
M4 + M5	33.8	− 47.6 (− 47.3)
TS6	35.3	− 28.2 (− 26.4)
M6	38.2	− 103.6 (− 99.0)
M7 + OH·	34.3	− 55.3 (− 54.6)
TS7	35.9	3.0 (5.4)
M8 + O$_2$ ($^1\Delta$)	35.8	− 52.1 (− 49.8)

[a] Obtained from CASSCF/6 – 31G(d) harmonic vibrational frequencies scaled by 0.8929. [b] ZPVE corrected values are given in parentheses. [c] The energy barriers, relative to **M1** (POZ) for the key structures **TS4**, **TS5**, **TS6** and **TS7** are computed to be 21.7, 24.7, 27.0 and 58.2 kcal mol^{-1}, respectively at the CCSD(T) level of theory and 14.4, 17.0, 23.0 and 55.5 kcal mol^{-1}, respectively at the CASPT2 level of theory.

stability of the van der Waals complex would be 0.74 kcal mol^{-1},[68] we can conclude that the computed activation energy should be about 5.8 kcal mol^{-1}, which is comparable with the experimental estimates (in the 4.2 – 5.8 kcal mol^{-1} range)[27] and other theoretical determinations (in the 2.5 – 5.5 kcal mol^{-1} range).[72]

Due to the large exothermicity involved, the formation of POZ turns out to be the rate-determining step for the whole ethylene ozonolysis.

Cleavage of ethylene POZ: We have found two different paths for the cleavage of ethylene POZ (**M1**), by a concerted and a stepwise mechanism respectively. The concerted mechanism leads to the Criegee intermediates, which have been discussed in the literature.[14, 22, 29] The stepwise path begins with the cleavage of the O – O bond leading to the biradical OCH$_2$CH$_2$OO, which in turn decomposes into different molecular fragments. Figure 2 shows a schematic potential energy level diagram for the decomposition of POZ.
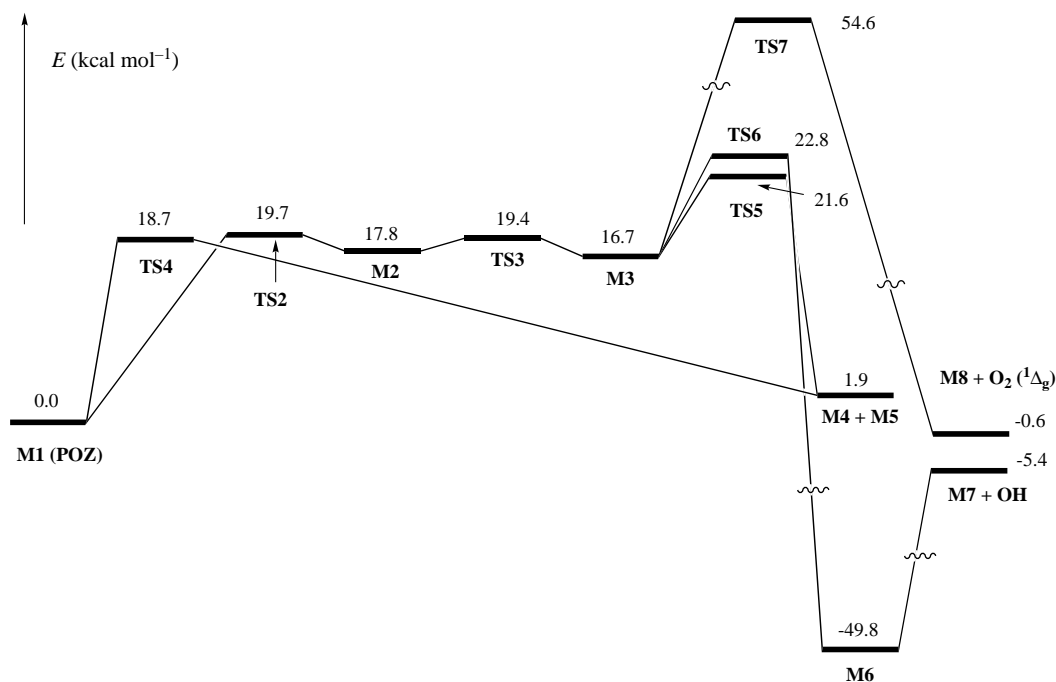

Figure 2. Schematic potential energy diagram showing the relative energies of the stationary points involved in the POZ cleavage. Energy values were obtained from ZPVE-corrected CCSD(T)/6 – 311G(2d,2p) energies.

The CASSCF geometries of the Criegee intermediates are taken from previous work.[13]

The geometric parameters of the transition structure (**TS4** in Figure 3) for the concerted POZ decomposition agree qualitatively with other theoretical results[14,75] except for the O1–O5 bond length, which is predicted by the CASSCF

approach to be more than 0.3 Å longer. The computed activation energy at 0 K is 21.7 kcal mol^{-1} (18.7 kcal mol^{-1} taking into account the ZPVE corrections) is also comparable with other results from the literature[14] (Figure 2). The Criegee intermediates (carbonyl oxide **M4** and formaldehyde **M5**) are computed to be 1.9 kcal mol^{-1} higher energetically
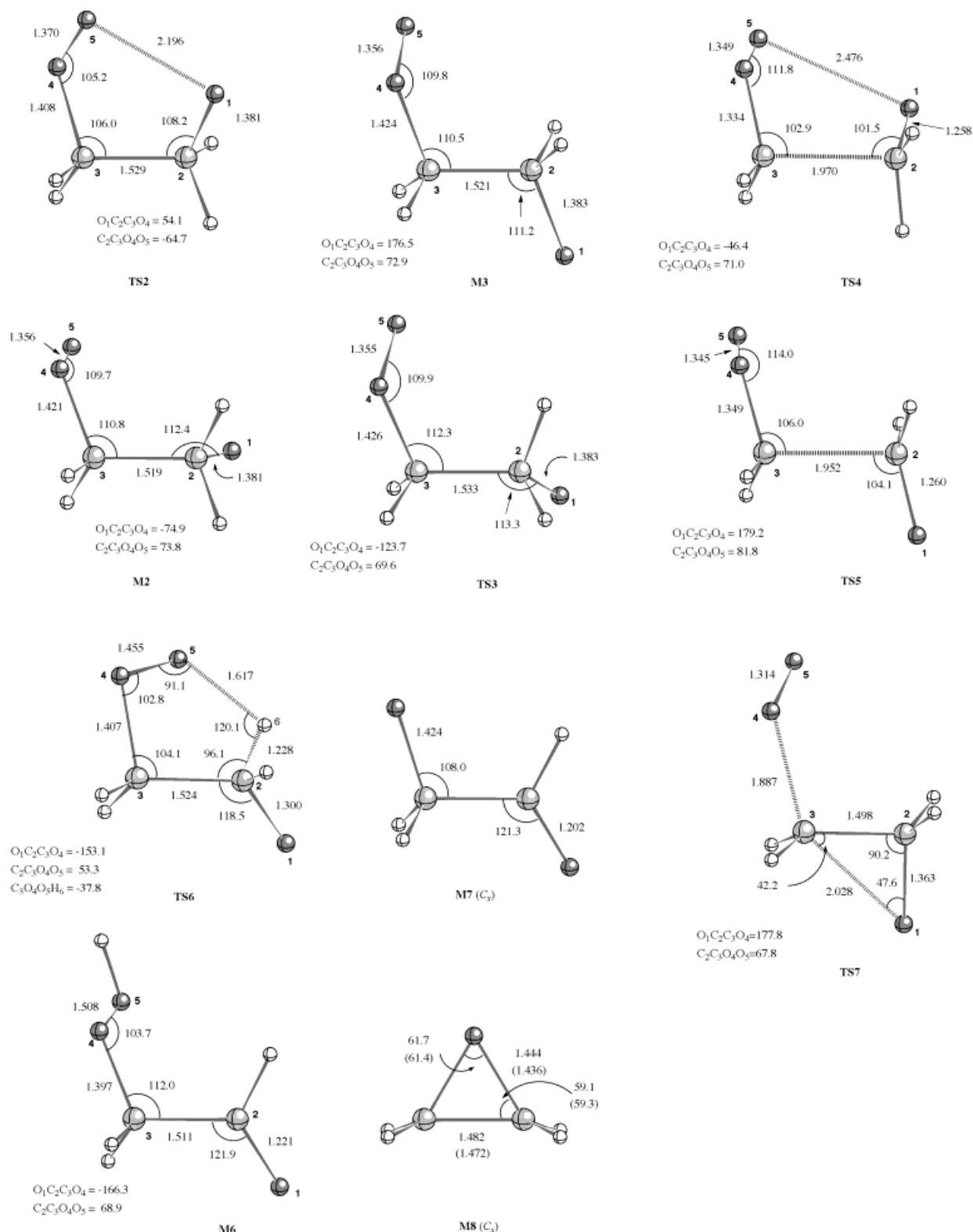

Figure 3. Selected geometric parameters of the CASSCF/6-31G(d)-optimized structures for the stationary points involved in the ethylene POZ cleavage. Distances are given in ångstroms and angles in degrees.

than POZ, so that the global process takes place without a significant energy change.

Regarding the stepwise mechanism, the transition structure for the first step of the POZ decomposition is **TS2** and we have found two rotational isomers (**M2** and **M3**) of OCH$_2$-CH$_2$OO that are connected through **TS3**. Structures **TS2**, **M2**, **TS3** and **M3** have similar geometric parameters (Figure 3). The cleavage of the O–O bond in POZ (compared with **M1** in Figure 1) leads to a shortening by 0.12 Å of the O–O bond and a shortening by 0.7 Å of the aldehyde C–O bond and an increase in the O-O-C-C dihedral angle of about 43°. These geometric changes indicate (O–O) π bond formation in the biradical structures. The formation of this π bond is allowed because after the relaxation of the O-O-C-C dihedral angle, the lone pairs of the two oxygen atoms overlap. Figure 2 and Table 1 show that the energy barrier is computed to be 19.7 kcal mol^{-1} at 0 K, and the biradical structures **M2** and **M3** are calculated to lie 17.8 and 16.7 kcal mol^{-1}, respectively, higher in energy than POZ, the *anti* isomer **M3** being around 1.0 kcal mol^{-1} more stable energetically than **M2**. The calculated energy barrier for the conformational change from **M2** to **M3** is 1.6 kcal mol^{-1}.

The next step of the reaction is the decomposition of the biradical intermediate **M3**. As schematized in Figure 2, we have found three different routes for the **M3** cleavage.

One possible route is decomposition through scission of the C–C bond to yield the Criegee intermediates (carbonyl oxide **M4** + formaldehyde **M5**). **TS5** is the transition structure connecting **M3** with **M4** + **M5**. The geometric features of the transition state include a C–C bond length of 1.970 Å and a reduction of both C–O bonds relative to the biradical **M2** and **M3** structures (by 0.12 Å in the formaldehyde moiety and 0.09 Å in the carbonyl oxide moiety). Thus, the C–O and O–O bond lengths resemble very closely those of the final carbonyl products.[13] These geometric changes indicate that the (C–O) π bond of both products is being formed at the same time as the C–C bond is being broken. The energy barrier for the scission of the C–C bond in **M3** is 4.9 kcal mol^{-1} (Table 1 and Figure 2) and the global activation energy at 0 K for the decomposition of POZ (**M1**) into the Criegee intermediates (**M4** and **M5**) through **TS5** is 21.6 kcal mol^{-1}, which is about 3 kcal mol^{-1} higher than that for the concerted path (via **TS4**); we therefore conclude that the energy barrier for the concerted path is lower than that of the stepwise mechanism.

Another route for the biradical structure **M3** leads to hydroperoxyacetaldehyde (**M6**), by hydrogen atom 1,4-migration from carbon to oxygen. The transition structure found for this isomerization (**TS6**) is a five-membered ring where the migrating hydrogen atom is linked to the carbon and oxygen atoms through the long bond lengths $R(CH) = 1.228$ Å and $R(OH) = 1.617$ Å. The O4–O5 bond length is computed to be 1.455 Å, which is about 0.1 Å longer than the corresponding distance in **M3**, and the O-O-C-C and H-C-C-O dihedral angles are $-53.3°$ and $40.6°$, respectively. It is also interesting to compare the geometric parameters of **TS6** with those of the transition structure for the tautomerization of acetaldehyde carbonyl oxide to hydroperoxyethylene,[13] which is a nearly planar five-membered ring having O–H and C–H bond

lengths of 1.322 and 1.382 Å, respectively. These differences reflect the distinct electronic structure of the COO moieties in the two transition structures. Thus, in the tautomerization of acetaldehyde carbonyl oxide to hydroperoxyethylene [13] the carbon atom is sp^2-hybridized and the π bond is delocalized on the COO moiety, whereas in **TS6** the carbon atom has sp^3 hybridization.

The computed energy barrier for the hydrogen atom migration in **M3** is 6.1 kcal mol^{-1} and the global barrier for the conversion of POZ (**M1**) to **M6** is computed to be 22.8 kcal mol^{-1}. This energy barrier is about 1 kcal mol^{-1} higher than that calculated for the decomposition of **M1** into the Criegee intermediates through **TS5**. In any case, we can conclude that, since POZ is formed with an excess of energy, **M6** will also be formed in the gas-phase ozonolysis of ethylene. Our calculations also indicate that the conversion of POZ (**M1**) to hydroperoxyacetaldehyde (**M6**) is exothermic by 49.8 kcal mol^{-1}. Despite the relatively low energy computed for **M6**, there is no experimental evidence recorded in the literature for the formation of this compound. However, Atkinson and Finlayson,[15] in a mass spectrometric study of the *cis*-2-butene–ozone reaction, observed a peak at m/z 104 and considered that the most likely product corresponding to this peak was 3-hydroperoxybutanone. This compound is the analogue of **M6** in the ozonolysis of *cis*-2-butene and we believe that it could be formed through the same mechanism.

Furthermore, hydroperoxyacetaldehyde (**M6**) can also decompose into the radicals **M7** and OH. Table 1 and Figure 2 indicate that this decomposition is endothermic by about 44.4 kcal mol^{-1}. However, since **M6** is also formed with an excess of energy (about 79 kcal mol^{-1}), we conclude that OH radicals might be generated in the gas-phase ozonolysis of ethylene through this mechanism. Therefore, this pathway may also contribute to OH-radical production in the gas-phase ozonolysis of ethylene. This step could offer an explanation of the differences in the measured (8–12%) and predicted (2%) OH yields in ethylene ozonolysis.[4,12,14]

The third alternative route, decomposition of **M3** into oxirane (**M8**) and molecular oxygen in its excited $^1\Delta_g$ state, takes place through a concerted mechanism via **TS7** (Figure 3). The computed geometric parameters of oxirane (**M8**) agree quite well with the reported experimental values.[76] Figure 2 shows a value of 54.6 kcal mol^{-1} for the global energy barrier with respect to **M1**, which is therefore higher than the energy barriers calculated for the other two channels described above, implying that this process would not compete with them. Moreover, Table 1 also shows that **TS7** has about the same energy as **TS1**, in the first step of the ethylene ozonolysis. Therefore it is possible that small amounts of oxirane are produced in the gas-phase ozonolysis of ethylene through this mechanism. This result is consistent with the suggestion of Martinez et al.[25] that a peak at m/z 44 that they observed in the mass spectra of the ethylene–ozone reaction was probably due to acetaldehyde, but included a contribution from oxirane. Martinez et al. also suggested that a further peak at m/z 32 had a possible contribution from O$_2$ ($^1\Delta_g$). These peaks in the mass spectra were not assigned to any mechanism. Figure 2 also shows that the whole process occurs without a significant energy change (-0.6 kcal mol^{-1}). How-

ever, this value is underestimated by about 10 kcal mol^{-1}, since the CCSD(T) calculations on O_2 based on a UHF wavefunction of broken symmetry result in an O_2 ($^3\Sigma^- - ^1\Delta$) excitation energy of 10.1 kcal mol^{-1}, about 10 kcal mol^{-1} lower than the experimental value of 22.6 kcal mol^{-1}.[77]

It is also interesting to compare the magnitude of the computed CCSD(T) and CASPT2 energy barriers for the key structures **TS4**, **TS5**, **TS6** and **TS7**, relative to **M1** (POZ) (see footnote [c] in Table 1). Although the CASPT2 activation energies are between 3.3 and 7.7 kcal mol^{-1} lower than the corresponding CCSD(T) values, the relative ordering of the different energy barriers is maintained at both levels of theory.

The stepwise mechanism described above agrees well with the O'Neal – Blumstein mechanism for gas-phase ozone – olefin reactions.[78, 79] Our results also agree with the stepwise mechanism suggested by Wadt and Goddard[17] and Harding and Goddard,[19] who postulated several biradical intermediates in the course of POZ decomposition.

Formation of the ethylene SOZ (1,2,4-trioxolane): The reaction of carbonyl oxide with formaldehyde giving SOZ is a [4+2] cycloaddition. As one would expect, this reaction has many similarities to the formation of POZ (see above), since in both cases the reactants are isoelectronic. Thus, we have found the formation of a van der Waals complex (**M9**) in the reaction coordinate, prior the transition state (**TS8**) and the formation of SOZ (**M10**).

The C–O distances between the carbonyl oxide and formaldehyde are 3.084 and 2.872 Å, respectively, in the van der Waals complex **M9** (Figure 4), while the geometry of the two moieties is almost the same as that calculated for the separate reactants.[13] Since 6-31G(d) is a poor basis set to describe van der Waals complexes, we have also re-optimized **M9** at the same level of theory with the more flexible 6-311G(2d,2p) basis set. The results, shown in brackets in Figure 4, indicate that the latter basis set expansion does not lead to significant geometric changes. Table 2 and Figure 5 show that **M9** is 6.3 kcal mol^{-1} more stable than the reactants. Comparing the van der Waals complex **M9** with the dipole complex computed by Cremer and co-workers,[68] at the MP4 level of theory the latter is reported to be 8.9 kcal mol^{-1} less energetic than the separate components (carbonyl oxide and formaldehyde), a value that is close to the 7.3 kcal mol^{-1} computed for **M9** in this work (without considering the ZPVE corrections; see Table 2). Moreover, in the complex reported by Cremer et al., the separation of the two components is about 2.5 Å, in contrast to the distance of about 2.9 Å found in **M9**. We believe that the dipole complex reported by Cremer et al. and **M9** represent the same structure and that the differences in the computed distances between the two components (carbonyl oxide and formaldehyde) may be due to the different theoretical approaches used in the two calculations. In a later study, Cremer et al.[43] concluded that the MP4 method was not adequate to predict the carbonyl oxide geometry; this deficiency may have affected the calculated long-range interactions between carbonyl oxide and formaldehyde.

The most relevant geometric features of **TS8** are the lengths of the forming C–O bonds between the two moieties (about

2 Å) and a slight elongation (0.06 Å) in the O–O bond of the carbonyl oxide moiety. Thus the π bonds in the formaldehyde and carbonyl oxide moieties are retained. Previous experimental and theoretical studies[69, 80, 81] indicated that the most stable conformation of SOZ had C_2 symmetry. We have considered the ^1A state of this symmetric conformer (**M10**), which is characterized by the $10a^2 9b^2$ electronic configuration. The most relevant geometric parameters of the CASSCF-optimized structure for SOZ (**M10**) compare quite well with the reported experimental data obtained from microwave spectroscopy (R(OO) = 1.461 Å, R(C–O) = 1.412 Å, r(C–O) = 1.416 Å, $\angle$(O-C-O) = 105.5°, $\angle$(C-O-O) = 99.3° and $\angle$(C-O-C) = 104.8°).[80]

The results displayed in Table 2 and Figure 5 show that the SOZ formation from the Criegee intermediates is exothermic by 46.0 kcal mol^{-1}. Moreover, the energy of the transition structure is lower than that of the reactants by 4.4 kcal mol^{-1}, and the energy barrier with respect to the van der Waals complex is calculated to be 1.9 kcal mol^{-1}. From Table 2, the single-point QCISD(T)/6-311G(2d,2p) energies place **TS8** lower in energy than **M9**, but the relative energy order is changed after the ZPVE corrections are included. This result is due to the different positions of the stationary points along the reaction coordinate at the CASSCF and QCISD(T) levels of theory. Our results clearly indicate that the reaction of carbonyl oxide with formaldehyde to yield SOZ is barrierless; that is, in the potential energy diagram, the transition state for the formation of SOZ lies below the reactants. Similar results were found by Ponec et al. in their study based on AM1 calculations.[37] These results are in accordance with the matrix experiments carried out at cryogenic temperatures by Samuni et al.,[36] who observed formation of POZ and SOZ at temperatures as low as 25 K and indicated that any contribution to the progress of the reaction from temperatures lower than 30 K could be neither neglected nor quantified.

Cleavage of the ethylene SOZ: The decomposition of SOZ takes place by a stepwise mechanism and shows a pattern similar to that found for the decomposition of POZ discussed above. The first step is the cleavage of the O–O bond yielding the biradical OCH_2OCH_2O. The second step is the decomposition of this biradical.

The cleavage of the O–O bond of SOZ is a symmetrical process, so the C_2 symmetry of **M10** is retained in the transition structure (**TS9**) and in the biradical (**M11**). Figure 5 shows that the computed energy barrier is 28.8 kcal mol^{-1} and the process is endothermic by 24.1 kcal mol^{-1}. We have found another rotational isomer of OCH_2OCH_2O (**M12**), which is linked to **M11** through **TS10**. The corresponding energy barrier is 3.1 kcal mol^{-1} (Figure 5 and Table 2). We observed very little change in the geometric parameters relative to SOZ (Figure 4). The only remarkable differences are a shortening by 0.07 Å of the C–O bond and an increase of about 10° in the O-C-O and C-O-C angles.

Figure 5 shows two different fates for the cleavage of the biradical intermediates **M11** and **M12** in the second step.

One alternative is the cleavage of the O3–C4 bond in **M11**, forming dioxymethane (**M13**) + formaldehyde (**M5**). In the
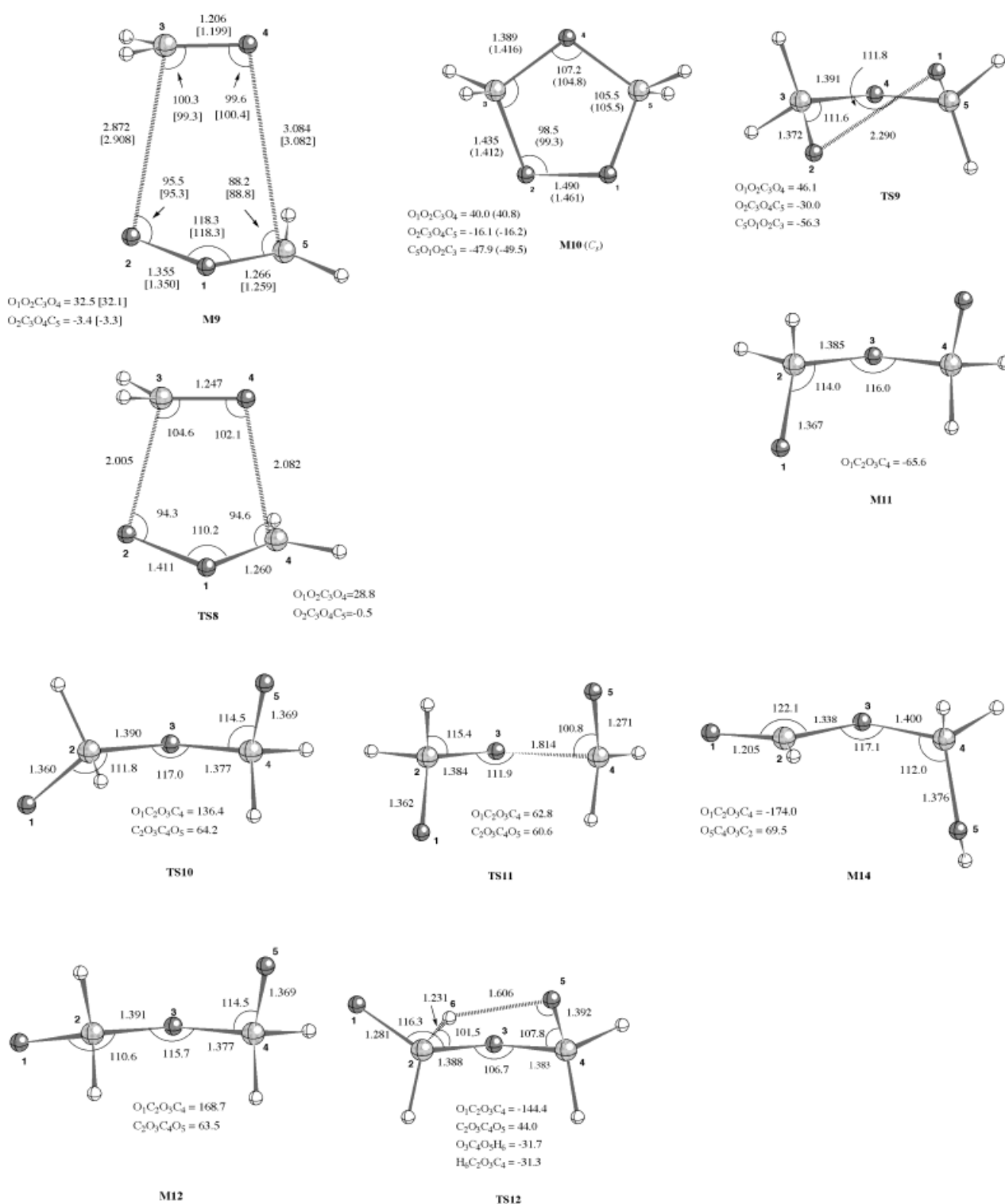
Figure 4. Selected geometric parameters of the CASSCF/6-31G(d)-optimized structures for the stationary points involved in the formation and cleavage of ethylene SOZ. Distances are given in ångstroms and angles in degrees. Values in square brackets correspond to parameters optimized by using the 6–311G(2d,2p) basis set. Values in parentheses correspond to experimental data.

corresponding transition structure (**TS11** in Figure 4), we observe that the C–O bond that is being broken is 1.814 Å long, while the C–O bond length in the formaldehyde moiety is reduced by 0.16 Å relative to the corresponding bond in SOZ. The CASSCF-optimized geometric parameters of dioxymethane (**M13**) are in very good agreement with those

reported previously in the literature.[40, 44] Figure 5 shows that the energy barrier is 24.6 kcal mol⁻¹. The products are computed to be 33.3 kcal mol⁻¹ higher in energy than SOZ and the calculated global energy barrier between **TS11** and SOZ is 48.7 kcal mol⁻¹. That is, **TS11** is 2.7 kcal mol⁻¹ higher in energy than the Criegee intermediates **M4** + **M5** (see also

Table 2. Zero point vibrational energies (ZPVE,[kcal mol^{-1}])[a] and relative energies (E [kcal mol^{-1}])[b,c] calculated for the CASSCF/6–31G(d)-optimized structures involved in the formation and decomposition of the ethylene SOZ.

Compound	ZPVE	E QCISD(T)/ 6–311G(2d,2p)
M4 + M5	33.8	0.0 (0.0)
M9	34.8	−7.3 (−6.3)
TS8	37.8	−8.4 (−4.4)
M10 (SOZ)	41.0	−53.2 (−46.0)
TS9	39.6	−23.0 (−17.2)
M11	39.4	−27.5 (−21.9)
TS10	39.0	−23.9 (−18.8)
M12	39.1	−24.2 (−19.0)
TS11	37.1	−0.3 (2.7)
M13 + M5	33.2	−12.1 (−12.7)
TS12	36.6	−16.1 (−13.4)
M14	40.7	−125.1 (−118.2)

[a] Obtained from CASSCF/6–31G(d) harmonic vibrational frequencies scaled by 0.8929. [b] ZPVE-corrected values are given in parentheses. [c] The energy barriers, relative to **M10** (SOZ), for the key structures **TS11** and **TS12** are computed to be 52.9 and 37.1 kcal mol^{-1} at the QCISD(T) level of theory and 57.3 and 26.4 kcal mol^{-1} at the CASPT2 level of theory.

Table 2 and Figure 5). Consequently, very little SOZ will decompose through this channel.

The second possible fate is the formation of hydroxymethyl formate (**M14**) through an hydrogen atom 1,4-migration from carbon to oxygen in **M12**. The transition structure for this rearrangement (**TS12**) corresponds to a five-membered ring, in which the migrating hydrogen atom is linked to the carbon and oxygen atoms through the long bond lengths $R(C-H) = 1.231$ Å and $R(O-H) = 1.606$ Å. The O-C-O-C and H-C-O-C dihedral angles are 44.0° and −31.3°, respectively. This transition structure resembles very closely the transition structure **TS6** calculated for the cleavage of POZ. The

corresponding energy barrier is computed to be only 5.6 kcal mol^{-1}. Table 2 and Figure 5 show that the energy barrier of the global process, with respect to SOZ, is 32.6 kcal mol^{-1}, which is about 16 kcal mol^{-1} lower than that for the cleavage of the C−O bond leading to dioxymethane + formaldehyde. Moreover, the process is highly exothermic (72.2 kcal mol^{-1}). These values indicate that **M14** will be the major product of the SOZ cleavage. Hydroxymethyl formate was initially identified as a transitory product in the gas-phase ozonolysis of ethylene,[21, 26, 82] and was supposed to be formed as a product of the carbonyl oxide + formaldehyde reaction, but further experimental work indicated that this transitory product could be hydroperoxymethyl formate,[32, 33] although the mechanism for its formation is only speculative.[32]

The energy barriers for the key structures **TS11** and **TS12**, relative to **M10** (SOZ), computed at CASPT2 levels of theory, differ by 4.4 and 10.7 kcal mol^{-1} respectively from the QCISD(T) values (see footnote [c] in Table 2). Despite these energy discrepancies, the relative ordering of the different energy barriers is maintained; consequently, these results do not affect the reaction mechanism discussed above.

It is also interesting to compare the cleavage of POZ and SOZ (Figures 2 and 5, respectively). The lowest energy decomposition pathway for the POZ cleavage corresponds to the scission of the C−C bond that yields the Criegee intermediates, whereas for the SOZ cleavage it corresponds to the hydrogen atom 1,4-migration yielding hydroxymethyl formate; the decomposition pathway that produces dioxymethane + formaldehyde has a higher energy barrier. These differences may be rationalized by taking into account the facts that in the cleavage of POZ the scission of the O−O and C−C bonds is associated with the formation of π bonds in the carbonyl oxide moiety (which implies an sp$^3 \rightarrow$ sp^2 hybridization change), involving energy stabilization, whereas in the
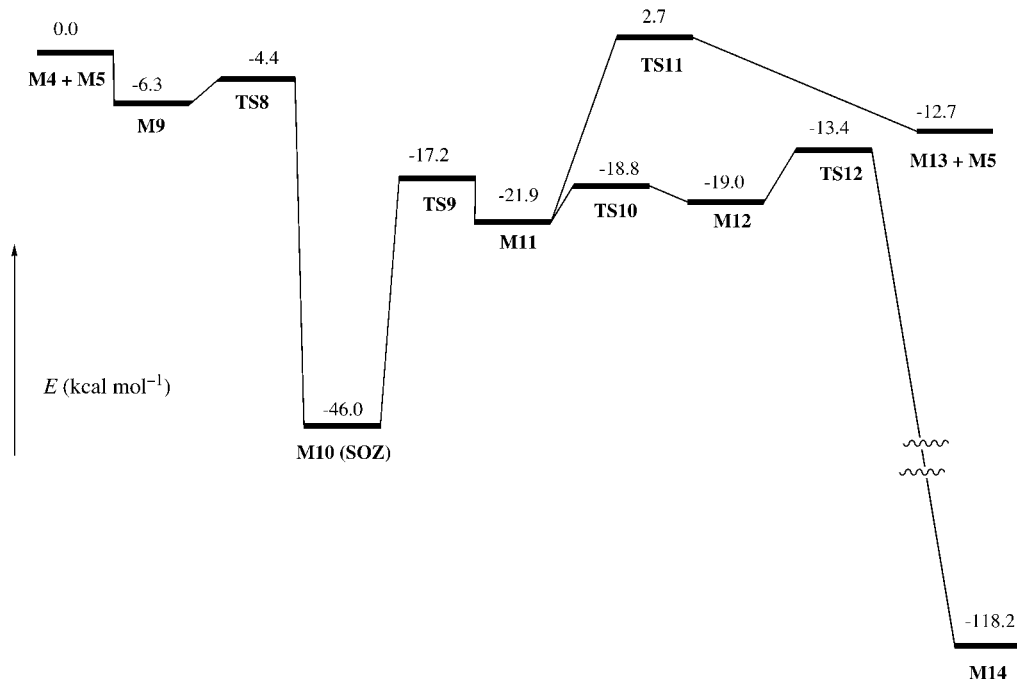

Figure 5. Schematic potential energy diagram showing the relative energies of the stationary points involved in the formation and cleavage of ethylene SOZ. Energy values were obtained from ZPVE-corrected QCISD(T)/6–311G(2d,2p) energies.
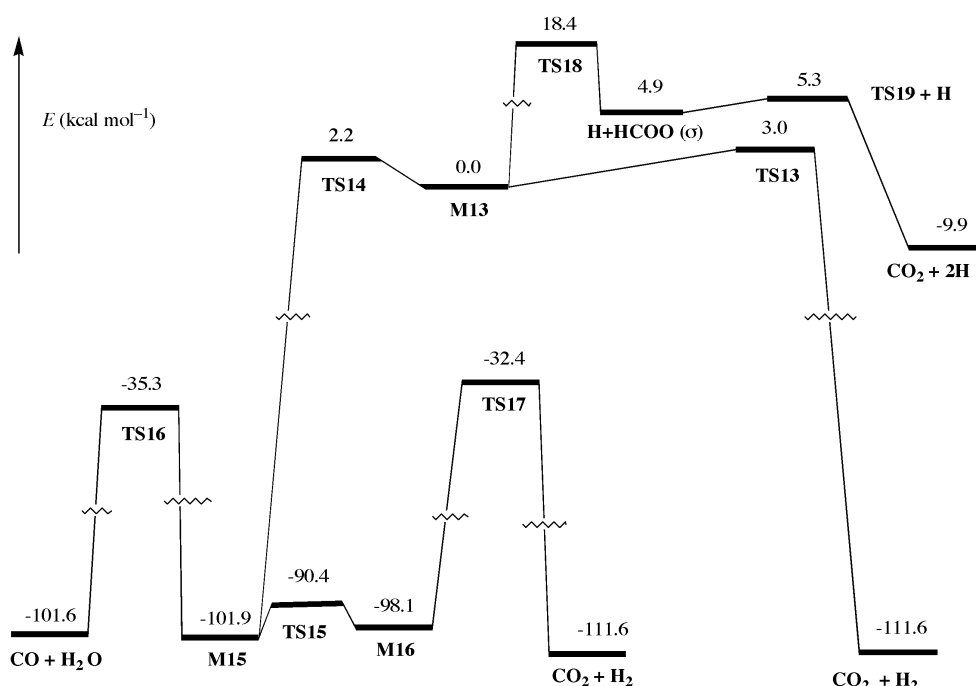
Figure 6. Schematic potential energy diagram showing the relative energies of the stationary points involved in the unimolecular decomposition of dioxymethane. Energy values were obtained from ZPVE-corrected QCISD(T)/6–311G(2d,2p) energies.

cleavage of SOZ the scission of the COO bond occurs without a hybridization change.

It should be noted that this stepwise mechanism contrasts with the concerted mechanism proposed on the basis of AM1 calculations.[29,37]

Unimolecular decomposition of dioxymethane: As mentioned in the previous section, dioxymethane (**M13**) can be formed in the cleavage of SOZ (**M10**), but it is also an intermediate in the unimolecular decomposition of carbonyl oxide (**M4**), which in turn is one of the products of POZ (**M1**) cleavage. This unimolecular process corresponds to the so-called ester channel, and involves the previous **M4** conversion to dioxirane.[6,8–10,13,39–44] There are three different pathways for the unimolecular decomposition of dioxymethane (**M13**): a) dissociation into H_2 and CO_2 in their ground states; b) isomerization to formic acid; and c) decomposition into H and HCOO radicals. Further, formic acid also decomposes into H_2, CO_2, H_2O and CO in their ground states, while HCOO decomposes into H + CO_2 in their ground states.

The dissociation of **M13** into H_2 and CO_2 takes place through a concerted mechanism through **TS13** (Figure 7) and involves synchronous breaking of the two C–H bonds and formation of the H–H bond; it has already been discussed extensively in the literature.[40,44] The calculated energy barrier is 3.0 kcal mol^{-1} and the dissociation process is computed to be exothermic by 111.6 kcal mol^{-1} (Figure 6 and Table 3). These values are in very good agreement with results reported from MRD-CI calculations.[44]

The geometry of the transition structure (**TS14**) for the isomerization of dioxymethane (**M13**) into *syn*-formic acid (**M15**) (Figure 7) shows a relative long O–H bond (1.691 Å), which is of the same order as those formed in the transition

structures **TS6** and **TS12**. The **M13**→**M15** isomerization is calculated to be exothermic by 101.9 kcal mol^{-1} with an energy barrier of 2.2 kcal mol^{-1}, which is only 0.8 kcal mol^{-1} lower than that calculated for the symmetrical dissociation of **M13** into CO_2 + H_2 (**TS13**) (see Figure 6 and Table 3). Therefore we conclude that the isomerization of **M13** to *syn*-formic acid and the dissociation of **M13** into CO_2 + H_2 are competitive processes.

Since formic acid is formed with an excess of energy, it can undergo a further unimolecular decomposition yielding CO_2, H_2, CO and H_2O. Figure 6 and Table 3 show that the *syn* isomer of formic acid (**M15**) is energetically more stable than the *anti* isomer (**M16**) by 3.8 kcal mol^{-1}. The *syn–anti* interconversion (**TS15**) takes place through rotation of the COH plane with a computed energy barrier of 11.5 kcal mol^{-1}. Dissociation of *syn*-formic acid (**M15**) into CO + H_2O takes place without a significant energy change (0.3 kcal mol^{-1}), while the dissociation of *anti*-formic acid (**M16**) into CO_2 + H_2 is slightly exothermic (-13.5 kcal mol^{-1}). The calculated energy barriers are 66.6 (**TS16**) and 65.7 kcal mol^{-1} (**TS17**) at 0 K, respectively, which are slightly lower than the energy barriers reported for the analogous processes in the unimolecular decomposition of acetic acid.[83]

The last alternative pathway for the unimolecular decomposition of dioxymethane is the dissociation into an hydrogen atom and a formyloxyl radical (HCOO) (Figure 6) through the homolytic cleavage of the C–H bond, which involves a computed energy barrier of 18.4 kcal mol^{-1} (Table 3 and Figure 6). This value is about 15 kcal mol^{-1} higher than the energy barriers computed for the two decomposition paths discussed above, and the process is calculated to be endothermic by 4.9 kcal mol^{-1}. Among the geometric parameters of the corresponding transition state (**TS18,** Figure 7), the
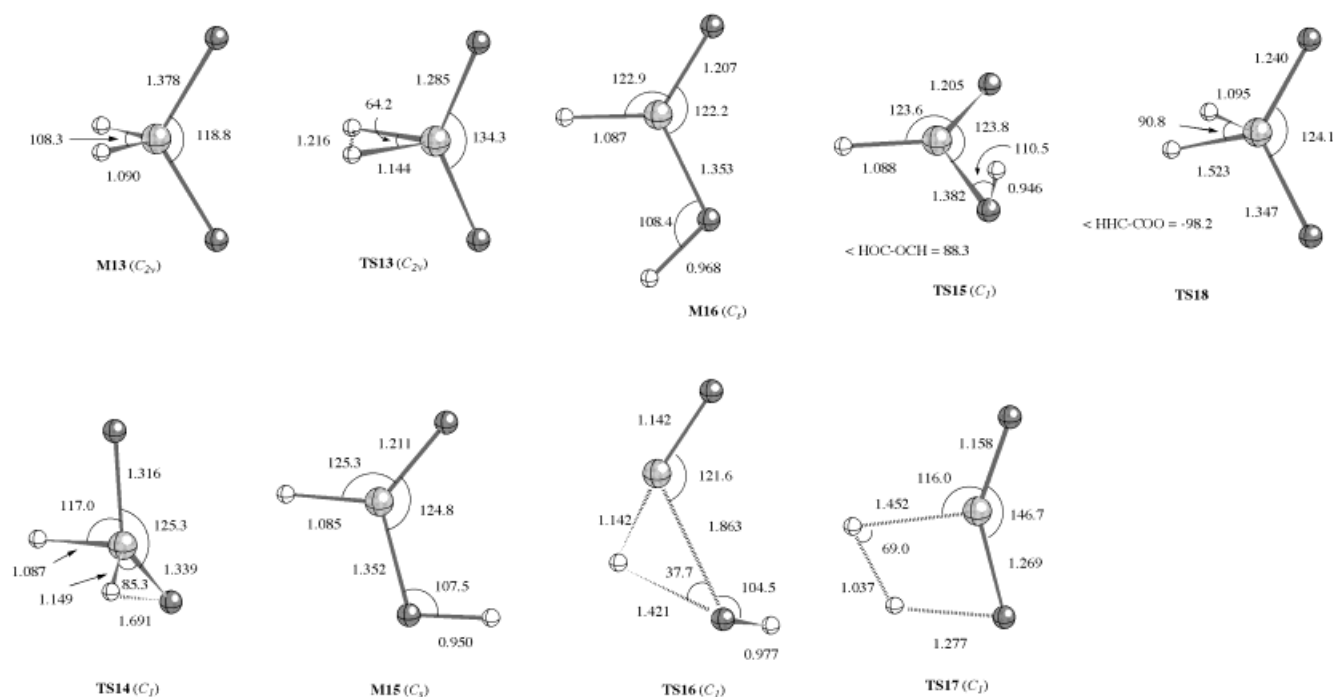
Figure 7. Selected geometric parameters of the CASSCF/6-31G(d,p)-optimized structures for the stationary points involved in the unimolecular decomposition of dioxymethane. Distances are given in ångstroms and angles in degrees.

Table 3. Zero point vibrational energies (ZPVE,[kcal mol^{-1}])[a] and relative energies (E [kcal mol^{-1}])[b] calculated for the CASSCF/6–31G(d,p)-optimized structures involved in the decomposition of dioxymethane.

Compound	ZPVE	E QCISD(T)/ 6–311G(2d,2p)
M13	17.4	0.0 (0.0)
TS13	14.9	5.5 (3.0)
CO$_2$ + H$_2$	11.6	− 105.8 (− 111.6)
TS14	15.9	3.7 (2.2)
M15	20.3	− 104.8 (− 101.9)
TS18	13.5	22.3 (18.4)
H + HCO$_2$[c]	10.9	11.4 (4.9)
TS15	18.8	− 91.8 (− 90.4)
M16	19.6	− 100.3 (− 98.1)
TS16	15.3	− 33.2 (− 35.3)
CO + H$_2$O	14.8	− 99.0 (− 101.6)
TS17	14.0	− 29.0 (− 32.4)
TS19 + H	6.5	16.2 (5.3)
CO$_2$ + 2H	5.9	1.6 (− 9.9)

[a] Obtained from CASSCF/6–31G(d,p) harmonic vibrational frequencies scaled by 0.8929. [b] Corrected values are given in parentheses. [c] Relative to ^{2}B$_2$ state.

bond length (1.523 Å) calculated for the breaking C–H bond and the different lengths of the C–O bonds are noteworthy: a symmetrical (C_s) transition structure might have been expected, with the homolytic cleavage of the C–H bond taking place in the symmetry plane of the molecule, but we believe that the asymmetrical structure of **TS18** may be due to the well-known doublet instability of the formyloxyl radical (HCOO) wavefunction.[84–86] Moreover, the COO moiety of **TS18** resembles very closely the structure of the ^{2}A′ electronic state of HCOO.[75,86,87]

Since the structure of the HCOO radical has received much attention in the literature,[84–90] our results will be only briefly

discussed here. The dissociation of the HCOO radical into H and CO$_2$, which has also been studied theoretically by Feller et al.,[84] is undergone by the so-called σ radical of HCOO, which has two low-lying electronic states of C_{2v} symmetry, namely ^{2}B$_2$ and ^{2}A$_1$. In addition, these two states yield the ^{2}A′ state after lowering the molecular symmetry to the C_s group. Our CASSCF[75]-optimized geometric parameters and relative energies are comparable with other results from ab initio calculations.[84,86,87] Our QCISD(T) calculation for the transition structure for the hydrogen atom loss from HCOO (**TS19**, Figure 6) predicts an energy barrier of 4.9 kcal mol^{-1} at 0 K, which is about 5 kcal mol^{-1} lower than that predicted by Feller et al.[84] Inclusion of the ZPVE corrections lowers this energy barrier to only 0.4 kcal mol^{-1}. It should be noted that the hydrogen atom loss is exothermic by 14.8 kcal mol^{-1}.

From the energy barrier heights in Figure 6 one may infer that the yield of CO$_2$ obtained through this process should be slightly greater than that of CO, which contrasts with the measured yields of these products in gas-phase ethylene ozonolysis.[2,6,21,39,82] However, Neeb et al.[39] recently concluded that a fraction of the CO produced in ethylene ozonolysis is due to a bimolecular reaction other than H$_2$COO unimolecular decomposition.

Conclusions

From our theoretical study of the gas-phase ozone–ethylene reaction, the principal trends of the mechanism are displayed in Scheme 1; for completeness, we have also included the main features of the unimolecular decomposition of carbonyl oxide, taken from other theoretical work reported in the
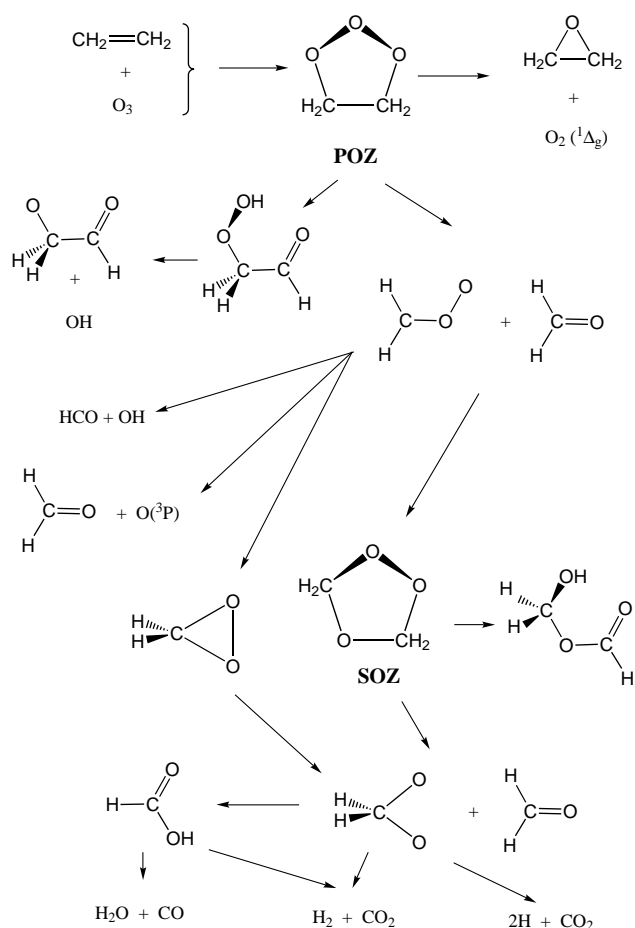
Scheme 1.

literature.[11,13,40–44] From the results obtained in the present investigation we emphasize the following important points:

1) The formation of POZ from the ozone – ethylene reaction is computed to be exothermic by 49.2 kcal mol^{-1} with an energy barrier of 5.0 kcal mol^{-1} at 0 K. These values are in agreement with experimental estimates and other theoretical results from the literature.[14,23,27,29,72] The optimized geometric parameters of the POZ are comparable with the reported experimental values.[71]

2) Our calculations indicate two pathways for the POZ cleavage: a concerted and a stepwise mechanism. The concerted mechanism leads to the formation of the Criegee intermediates (**M4** + **M5**) with a computed activation energy of 18.7 kcal mol^{-1} at 0 K, in agreement with other results from the literature.[14] This is the lowest energy path for the POZ decomposition. The first step of the stepwise mechanism involves the cleavage of the O – O bond yielding the two isomers **M2** and **M3**, which possess a strong biradical character. We have found three different fates for these biradicals, namely: a) the Criegee intermediates, the formation of which involves a scission of the C – C bond in **M3**; b) hydroperoxyacetaldehyde (**M6**), which is formed after tautomerization of **M3**; c) oxirane (**M8**) + molecular oxygen in the $^1\Delta_g$ excited state through a concerted mechanism from **M3**. The computed global energy barriers for the decomposition of POZ are 21.6 kcal mol^{-1} for the decomposition into the

Criegee intermediates and 22.8 kcal mol^{-1} for the tautomerization to **M6**. The energy barrier for the decomposition into oxirane + molecular oxygen in the $^1\Delta_g$ excited state is much higher in energy and only very little oxirane should be formed through this process. Since POZ is formed with an excess of energy, the other three paths will be active in the gas-phase ozonolysis of ethylene. Moreover, hydroperoxyacetaldehyde is formed with an excess of energy and can dissociate into the OH and CH$_2$OCHO radicals. Therefore this step can contribute to the release of OH radicals to the atmosphere.

3) The mechanism of formation of SOZ from the Criegee intermediates is analogous to that of POZ. The carbonyl oxide + formaldehyde reaction involves the formation of a van der Waals complex on the reaction coordinate prior to the transition state and SOZ. The van der Waals complex lies 6.3 kcal mol^{-1} below the energy of the reactants. The reaction is computed to be exothermic by 46.0 kcal mol^{-1} and the transition state has a lower energy than the reactants. This implies that the carbonyl oxide + formaldehyde reaction is barrierless. The optimized geometric parameters of SOZ agree quite well with the reported experimental values.[80]

4) The cleavage of SOZ follows a stepwise mechanism with the formation of a biradical intermediate with two isomers, **M10** and **M11**. The second step involves two different fates: a) dissociation into dioxymethane + formaldehyde, which is endothermic; b) tautomerization to yield hydroxymethyl formate (highly exothermic). The computed global energy barriers for the decomposition of SOZ are 48.7 kcal mol^{-1} for the dissociation into dioxymethane (**M13**) + formaldehyde (**M5**), and 32.6 kcal mol^{-1} for the tautomerization yielding hydroximethyl formate (**M14**). This stepwise mechanism contrasts with the concerted mechanism proposed on the basis of AM1 calculations.[29,37]

5) We have also considered the unimolecular decomposition of dioxymethane. This compound can be formed in the cleavage of SOZ but it is also an intermediate in the unimolecular decomposition of carbonyl oxide, which in turn is one of the products from the POZ cleavage. The symmetrical dissociation into CO$_2$ and H$_2$ is calculated to be exothermic by 111.6 kcal mol^{-1} with an activation energy at 0 K of only 3.0 kcal mol^{-1}. The isomerization to formic acid is also highly exothermic (101.9 kcal mol^{-1}) and the computed activation energy at 0 K is even lower (2.2 kcal mol^{-1}), which means that the two processes are competitive. Since formic acid is formed with an excess of energy, it can also decompose into CO$_2$ + H$_2$ (with an activation energy of 69.5 kcal mol^{-1} at 0 K) and CO + H$_2$O (with an activation energy of 66.6 kcal mol^{-1} at 0 K). Dioxymethane can also undergo a radical decomposition yielding H and HCOO radicals. This process is endothermic by 4.9 kcal mol^{-1} and the corresponding energy barrier is calculated to be 18.4 kcal mol^{-1} at 0 K. The energy barrier for the dissociation of HCOO into H + CO$_2$ has been calculated to be only 0.4 kcal mol^{-1} at 0 K.

[1] R. Atkinson, W. P. L. Carter, *Chem. Rev.* **1984**, *84*, 437 – 470.

[2] R. Atkinson, *Atmos. Environ.* **1990**, *24A*, 1 – 41.

[3] W. P. L. Carter, *Atmos. Environ.* **1990**, *24A*, 481 – 518.

[4] R. Atkinson, S. M. Aschmann, *Environ. Sci. Technol.* **1993**, *27*, 1357 – 1363.

[5] R. Criegee, *Angew. Chem.* **1975**, *87*, 765 – 771; *Angew. Chem. Int. Ed. Engl.* **1975**, *14*, 745 – 752.

[6] J. T. Herron, E. Huie, *J. Am. Chem. Soc.* **1977**, *99*, 5430 – 5435.

[7] S. Gäb, E. Hellpointner, W. V. Turner, F. Korte, *Nature (London)* **1985**, *316*, 535 – 536.

[8] H. Niki, P. D. Maker, C. M. Savage, L. P. Breitenbach, M. D. Hurley, *J. Phys. Chem.* **1987**, *91*, 941 – 946.

[9] R. I. Martinez, J. T. Herron, *J. Phys. Chem.* **1987**, *91*, 946 – 953.

[10] R. I. Martinez, J. T. Herron, *J. Phys. Chem.* **1988**, *92*, 4644 – 4648.

[11] R. Gutbrod, R. N. Schindler, E. Kraka, D. Cremer, *Chem. Phys. Lett.* **1996**, *252*, 221 – 229.

[12] R. Gutbrod, E. Kraka, R. N. Schindler, D. Cremer, *J. Am. Chem. Soc.* **1997**, *119*, 7330 – 7342.

[13] J. M. Anglada, J. M. Bofill, S. Olivella, A. Solé, *J. Am. Chem. Soc.* **1996**, *118*, 4636 – 4647.

[14] M. Olzmann, E. Kraka, D. Cremer, R. Gutbrod, S. Andersson, *J. Phys. Chem.* **1997**, *101*, 9421 – 9429.

[15] R. Atkinson, B. J. Finlayson, J. N. Pitts Jr., *J. Am. Chem. Soc.* **1973**, *95*, 7592 – 7599.

[16] B. J. Finlayson, *J. Am. Chem. Soc.* **1974**, *76*, 5356 – 5367.

[17] W. R. Wadt, W. A. Goddard III, *J. Am. Chem. Soc.* **1975**, *97*, 3004 – 3021.

[18] P. C. Hiberty, *J. Am. Chem. Soc.* **1976**, *98*, 6088 – 6092.

[19] L. B. Harding, W. A. Goddard III, *J. Am. Chem. Soc.* **1978**, *100*, 7180 – 7188.

[20] G. D. Fong, R. L. Kuczkowski, *J. Am. Chem. Soc.* **1980**, *102*, 4763 – 4768.

[21] F. Su, G. Calvert, H. H. Shaw, *J. Phys. Chem.* **1980**, *84*, 239 – 246.

[22] D. Cremer, *J. Am. Chem. Soc.* **1981**, *103*, 3619 – 3626.

[23] D. Cremer, *J. Am. Chem. Soc.* **1981**, *103*, 3627 – 3633.

[24] D. Cremer, *J. Am. Chem. Soc.* **1981**, *103*, 3633 – 3638.

[25] R. I. Martinez, J. T. Herron, R. E. Huie, *J. Am. Chem. Soc.* **1981**, *103*, 3807 – 3820.

[26] H. Niki, P. D. Maker, C. M. Savage, L. P. Breitenbach, *J. Phys. Chem.* **1981**, *85*, 1024 – 1027.

[27] C. S. Kan, J. G. Calvert, J. H. Shaw, *J. Phys. Chem.* **1981**, *85*, 2359 – 2363.

[28] D. Grosjean, *Environ. Sci. Technol.* **1990**, *24*, 1428 – 1432.

[29] M. J. S. Dewar, J. C. Hwang, D. R. Kuhn, *J. Am. Chem. Soc.* **1991**, *113*, 735 – 741.

[30] C. R. Greene, R. Atkinson, *Int. J. Chem. Kin.* **1992**, *24*, 803 – 811.

[31] D. Grosjean, E. Grosjean, E. L. Williams II, *Environ. Sci. Technol.* **1994**, *28*, 186 – 196.

[32] P. Neeb, O. Horie, G. K. Moortgat, *Int. J. Chem. Kin.* **1995**, *28*, 721 – 730.

[33] P. Neeb, O. Horie, G. K. Moortgat, *Tetrahedron Lett.* **1996**, *37*, 9297 – 9300.

[34] R. Atkinson, E. C. Tuazon, S. M. Aschmann, *Environ. Sci. Technol.* **1995**, *29*, 1860 – 1866.

[35] E. Grosjean, J. Bittercourt de Andrade, D. Grosjean, *Environ. Sci. Technol.* **1996**, *30*, 975 – 983.

[36] U. Samuni, R. Fraenkel, Y. Haas, R. Fajgar, J. Pola, *J. Am. Chem. Soc.* **1996**, *118*, 3687 – 3693.

[37] R. Ponec, G. Yuzhakov, Y. Haas, U. Samuni, *J. Org. Chem.* **1997**, *62*, 2757 – 2762.

[38] O. Horie, G. K. Moortgat, *Acc. Chem. Res.* **1998**, *31*, 387 – 396.

[39] P. Neeb, O. Horie, G. K. Moortgat, *J. Phys. Chem. A* **1998**, *102*, 6778 – 6785.

[40] G. Karlström, S. Engström, B. Jönsson, *Chem. Phys. Lett.* **1979**, *67*, 343 – 347.

[41] G. Karlström, B. O. Roos, *Chem. Phys. Lett.* **1981**, *79*, 416 – 420.

[42] R. D. Bach, J. L. Andrés, A. L. Owensby, H. B. Schlegel, J. J. W. McDouall, *J. Am. Chem. Soc.* **1992**, *114*, 7207 – 7217.

[43] D. Cremer, J. Gauss, E. Kraka, J. F. Stanton, R. J. Bertlett, *Chem. Phys. Lett.* **1993**, *209*, 547 – 556.

[44] J. M. Anglada, J. M. Bofill, S. Olivella, A. Solé, *J. Phys. Chem. A* **1998**, *19*, 3398 – 3406.

[45] B. O. Roos, *Adv. Chem. Phys.* **1987**, *69*, 399.

[46] J. Baker, *J. Comput. Chem.* **1986**, *7*, 385.

[47] J. Baker, *J. Comput. Chem.* **1987**, *8*, 563.

[48] J. M. Bofill, *J. Comput. Chem.* **1994**, *15*, 1 – 11.

[49] J. M. Anglada, J. M. Bofill, *Chem. Phys. Lett.* **1995**, *243*, 151 – 157.

[50] R. J. Buenker, S. D. Peyerimhoff, *Theoret. Chim. Acta* **1975**, *39*, 217 – 228.

[51] R. J. Buenker, S. D. Peyerimhoff, in *New Horizons of Quantum Chemistry, Vol. 35* (Eds: P. O. Lowdin, B. Pullman), D. Reidel, Dordrecht, **1983**, p. 183.

[52] R. J. Buenker, R. A. Philips, *J. Mol. Struct.: THEOCHEM* **1985**, *123*, 291.

[53] For O_3 the active space consists of 12 active electrons and nine active orbitals (CASSCF(12,9)). The active orbitals comprise three of a_1, one of a_2, two of b_1 and three of b_2 symmetry. For ethylene, a CASSCF(2,2) was selected, and the active orbitals correspond to the π and π^* orbitals. For **M1** and **TS1** a CASSCF(10,9) was chosen. The active orbitals are five of a' and four of a'' symmetry. For **TS2**, **M2**, **TS3**, **M3**, **TS4**, **TS5**, **TS6**, **TS7** and **M6** the active space selection procedure leads to a CASSCF(6,6) wavefunction. The geometries of **M4** and **M5** are taken from the literature (ref. [12]). For **M7** and **M8** the active space selection procedure leads to CASSCF(5,5) and CASSCF(8,8) wavefunctions, respectively. OH has been described by a Restricted Open Shell Hartree – Fock (ROHF) wavefunction and for $O_2(^1\Delta_g)$ the active space selection procedure leads to a CASSCF(8,6) wavefunction. The active space selection procedure leads to a CASSCF(8,7) for **M9**, **TS8**, and **M10**. The active orbitals are three of a and four of b symmetry, respectively. For **TS9**, **TS10**, **M11** and **M12** the active space consists of two active electrons and two active orbitals (CASSCF(2,2)) which correspond to the unpaired electrons. For **TS11**, **TS12** and **M14** the active space selection procedure leads to a CASSCF(4,4) wavefunction. For **M13** and **TS13** the active space selection procedure leads to a CASSCF(8,7) wavefunction. The active orbitals are two of a_1, one of a_2, two of b_1 and two of b_2 symmetry. For **TS14**, **M15**, **TS15**, **M16**, **TS16** and **TS17** the active space selection procedure leads to a CASSCF(10,9) wavefunction, similar to that employed in ref. 78. For **TS18** the active space consists of eight active electrons and eight active orbitals. For all structures of the HCOO σ radical ($^2B_2$, $^2A'$, $^2A_1$ and $^2A_1$ (**TS19**)), the active space selection procedure leads to a CASSCF(13,11) wavefunction, similar to that employed in ref. 81. For H_2O, CO and CO_2, the active space selection procedure leads to CASSCF(6,6), CASSCF(8,7) and CASSCF(12,9) wavefunctions, respectively.

[54] R. G. Parr, W. Yang, *Density-Functional Theory of Atoms and Molecules*, Oxford University Press, New York, **1989**.

[55] J. A. Pople, P. M. W. Gill, B. G. Johnson, *Chem. Phys. Lett.* **1992**, *199*, 557.

[56] B. G. Johnson, M. J. Frisch, *Chem. Phys. Lett.* **1993**, *216*, 133.

[57] A. D. Becke, *J. Chem. Phys.* **1993**, *98*, 5648.

[58] J. A. Pople, M. Head-Gordon, K. Raghavachari, *J. Chem. Phys.* **1987**, *87*, 5968 – 5975.

[59] L. A. Curtiss, K. Raghavachari, G. W. Trucks, J. A. Pople, *J. Chem. Phys.* **1991**, *94*, 7221.

[60] P. C. Hariharan, J. A. Pople, *Theoret. Chim. Acta* **1973**, *28*, 213.

[61] R. Krishnan, J. S. Binkley, R. Seeger, J. A. Pople, *J. Chem. Phys.* **1980**, *72*, 650.

[62] J. Cizek, *Adv. Chem. Phys.* **1969**, *14*, 35.

[63] G. E. Scuseria, H. F. Schaefer III, *J. Chem. Phys.* **1989**, *90*, 3700 – 3703.

[64] M. W. Schmidt, K. K. Baldrige, J. A. Boatz, J. H. Jensen, S. Koseki, M. S. Gordon, K. A. Nguyen, T. L. Windus, S. T. Elbert, *QCPE Bull.* **1990**, *10*, 52.

[65] M. J. Frisch, G. W. Trucks, H. B. Schlegel, P. M. W. Gill, B. G. Johnson, M. A. Robb, J. R. Cheeseman, T. Keith, G. A. Petersson, J. A.

Montgomery, K. Raghavachari, M. A. Al-Laham, V. G. Zakrzewski, J. V. Ortiz, J. B. Foresman, J. Cioslowski, B. B. Stefanov, A. Nanayak-kara, M. Challacombe, C. Y. Peng, P. Y. Ayala, W. Chen, M. W. Wong, J. L. Andres, E. S. Replogle, R. Gomperts, R. L. Martin, D. J. Fox, J. S. Binkley, D. J. Defrees, J. Baker, J. P. Stewart, M. Head-Gordon, C. Gonzalez, J. A. Pople, , Gaussian, Inc., Pittsburgh (PA), **1995**.

[66] K. Anderson, P. A. Malmqvist, B. O. Roos, *J. Chem. Phys.* **1992**, *96*, 1218.

[67] K. Anderson, M. P. Fülscher, R. Lindh, P. A. Malmqvist, J. Olsen, B. O. Roos, A. J. Sadlej, P. O. Widmark, University of Lund and IBM, Lund, Sweden, **1991**.

[68] C. W. Gillies, J. Z. Gillies, R. D. Suenram, F. J. Lovas, E. Kraka, D. Cremer, *J. Am. Chem. Soc.* **1991**, *113*, 2412 – 2421.

[69] D. Cremer, *J. Chem. Phys.* **1978**, *70*, 1898 – 1910.

[70] J. Zozom, C. W. Gillies, R. D. Suenram, F. J. Lovas, *Chem. Phys. Lett.* **1987**, *139*, 64 – 70.

[71] J. Z. Gillies, C. W. Gillies, R. D. Suenram, F. J. Lovas, *J. Am. Chem. Soc.* **1988**, *110*, 7991 – 7999.

[72] M. L. McKee, C. M. Rohlfing, *J. Am. Chem. Soc.* **1989**, *111*, 2497 – 2500.

[73] P. Borowski, M. Fülscher, P.-Å. Malmqvist, B. O. Roos, *Chem. Phys. Lett.* **1995**, *237*, 195 – 203.

[74] T. Tsuneda, H. Nakano, K. Hirao, *J. Chem. Phys.* **1995**, *103*, 6520 – 6528.

[75] See also the Supporting Information.

[76] G. Herzberg, *Electronic Spectra and Electronic Structure of Polya-tomic Molecules*, van Nostrand Reinhold, New York, **1966**.

[77] K. P. Huber, G. Herzberg, *Molecular Spectra and Molecular Structure.*, *Vol. 4*, van Nostrand, New York, **1979**.

[78] H. E. O'Neal, C. Blumstein, *Int. J. Chem. Kinet.* **1973**, *5*, 397.

[79] P. S. Bailey, *Ozonation in Organic Chemistry*, *Vol. 1*, Academic Press, New York, **1978**.

[80] R. L. Kuczkowski, C. W. Gillies, K. L. Gallaher, *J. Mol. Spectrosc.* **1976**, *60*, 361 – 372.

[81] R. L. Kuczkowski, *Acc. Chem. Res.* **1983**, *16*, 42 – 47.

[82] O. Horie, G. K. Moortgat, *Atmos. Environ.* **1991**, *25A*, 1881 – 1896.

[83] X. Duan, M. Page, *J. Am. Chem. Soc.* **1995**, *117*, 5114 – 5119.

[84] D. Feller, E. S. Huyser, W. T. Borden, E. R. Davidson, *J. Am. Chem. Soc.* **1983**, *105*, 1459 – 1466.

[85] A. D. McLean, B. H. Lengsfield III, J. Pacansky, Y. Ellinger, *J. Chem. Phys.* **1985**, *83*, 3567.

[86] A. Rauk, D. Yu, P. Borowski, B. O. Roos, *Chem. Phys.* **1995**, *197*, 73 – 80.

[87] A. Rauk, D. Yu, D. A. Armstrong, *J. Am. Chem. Soc.* **1994**, *116*, 8222 – 8228.

[88] S. D. Peyerimhoff, P. S. Skell, D. D. May, R. J. Buenker, *J. Am. Chem. Soc.* **1982**, *104*, 4515 – 4520.

[89] N. A. Burton, Y. Yamaguchi, I. L. Alberts, H. F. Schaefer III, *J. Chem. Phys.* **1991**, *95*, 7466.

[90] D. Yu, A. Rauk, D. A. Armstrong, *J. Phys. Chem.* **1992**, *96*, 6031.